ANALYTICAL AND FINITE ELEMENT ANALYSIS OF A NEW TRI-AXIAL PIEZOELECTRIC ACCELEROMETER

Ma-hui XU[1], Jian-yan WANG[1], Rui-hua HAN[1], Hui ZHOU[2,1], Hang GUO[1*]

[1]Pen-Tung Sah Institution of Micro-Nano Science and Technology, Xiamen University, Fujian, 361005, China
[2]School of Physical Science and Technology, Xiamen University, Fujian, 361005, China
[*]Corresponding author, E-mail: hangguo@xmu.edu.cn.

A new type of tri-axial piezoelectric accelerometer is proposed in this study. It consists of a seismic mass and four cantilever beams that is distributed in a shape of *X*. Analytical model and FEM analysis were conducted to study its charge sensitivity and the fundamental/first order resonance frequency in the Z-axis, X-axis and Y-axis direction. The errors between the calculated results from analytical model and that from the FEM analysis in ANSYS is about 8% for the charge sensitivity and 12% for the first-order resonance frequency. For a single chip with the same chip area, charge sensitivity of the proposed new *X*-shaped piezoelectric accelerometer is higher than that of the conventional cross-shaped piezoelectric accelerometer by 21%, which suggests that overall size of the accelerometer could be greatly reduced under the premise of meeting the design objectives.

Keywords: X type structure; Piezoelectric accelerometer; Charge sensitivity; Fundamental frequency; Bandwidth

1. INTRODUCTION

Micro accelerometers based on MEMS technology have been developed in recent decades, and they are widely used in aerospace navigation, automobile control, and biomedical instrumentation due to small size, effective cost, high performance and low power consumption [1]. Among various types of micro accelerometers, piezoresistive [2] and capacitive [3] approaches have attracted the most attention because of ease fabrication and high sensitivity. However, their application is far from satisfactory due to the inherent defect: for instance, piezoresistive sensing consumes inherently high power, whereas capacitive sensing requires elaborate electronics that is often power hungry. With advantages of low power consumption, wide bandwidth and high sensitivity, micro piezoelectric accelerometer has become a research hotspot [4].

In 1992, Yasunori Ohtsuki [5] put forward a structure of the ceramic based piezoelectric accelerometer. This conventional scale accelerometer could detect acceleration in two directions with just one detecting element used. But the sensitivity difference between two axes of this type piezoelectric accelerometer is very small. With the MEMS technology developed, many new progresses have been achieved and the cross-shaped micro piezoelectric accelerometer, as shown in Fig. 1(a), is adopted and investigated by many research groups [6-11]. In this structure, the piezoelectric material deposited on the cantilever beam was used as sensing element. It can detect the acceleration in tri-axis directions with a single mass block. In order to further raise the sensitivity of the MEMS-based accelerometers, we propose a new X-shaped micro piezoelectric accelerometer shown in Fig.1(b). For this new type accelerometer, the four cantilever beams connect between 4 corners of the mass block and the outer frame, instead of connecting between the middle of the four sides of the mass block and the outer frame for the cross-shaped accelerometer, leading to an great extension of the length of each cantilever beam, which is beneficial to increase the sensitivity of the accelerometer. Both theoretical and numerical study have been made, and based on these, the new X-shaped micro piezoelectric accelerometer has been designed and results showed that the charge sensitivity are significantly improved.

2. STRUCTURE OF MICRO PIEZOELECTRIC ACCELEROMETER

Structure of the X-shaped micro piezoelectric accelerometer is shown in Fig. 1(b), which comprises a seismic mass and four cantilever beams. Electrodes on the top of four cantilever beams are segmented into Z_1, Z_2, Z_3, Z_4, X_1, X_2, and Y_1 and Y_2. When acceleration in the direction of Z is applied, tensile stress is produced on the top half of the bimorph in X_1, X_2, Y_1 and Y_2; compressive stress is generated in Z_1–Z_4. Furthermore, there exists a finite voltage V_z between the parallel-connected Z_1–Z_4 and the electrode on the other face of the diaphragm, which results from the opposite stress distribution in the top and bottom halves of the bimorph. In addition, the voltage (V_x) between X_1 and X_2 and V_y between Y_1 and Y_2 is found to be zero, suggesting a net stress of zero between the two

978-1-5090-1189-6/16/$31.00 ©2016 IEEE

electrodes. When acceleration in the direction of X is applied, the seismic mass would rotate around Y-axis and meanwhile produces tensile stress in X_1 and Z_4 and compressive stress in Z_2 and X_2. It also produces shear stress in Y_1, Y_2, Z_1, and Z_3, which can be neglected. Thus, acceleration along X-axis direction produces a finite differential signal V_x, V_y and V_z. Both V_y and V_z are close to zero due to the zero net stress between Y_1 and Y_2, Z_1 and Z_3, respectively. This avoids the charge jamming of Y-axis direction and Z-axis direction on the detection of acceleration in X direction.

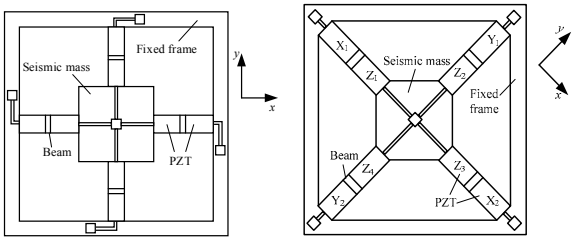

Figure1 Structure of two types of micro piezoelectric accelerometers. (a) Structure of the cross-shaped piezoelectric accelerometer. (b) Structure of the proposed new X-shaped piezoelectric accelerometer

3. ANALYTICAL MODEL AND FEM ANALYSIS

3.1. Analytical model

In order to predict the performance of the piezoelectric accelerometer, the charge sensitivity and the first order resonance frequency of the three axis double piezoelectric accelerometer are analyzed.

A. Charge sensitivity of Z-axis

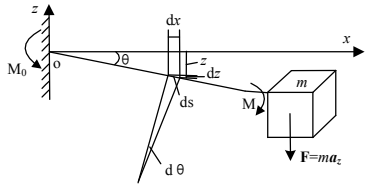

Figure 2 Simplified model with acceleration in the Z-axis direction.

Hypotheses should be put forward to conduct the model analysis: (1) Compared with the seismic mass, mass of the cantilever beam is very small and can be ignored; (2) As a rigid body, the seismic mass could be regarded as a mass point for the analysis; (3) PZT material and silicon cantilever have good elasticity and meet the Hooke law; (4) The thickness of electrodes on the top and bottom of PZT thin film could be ignored compared with that of the cantilever beams; (5) When acceleration in the direction of Z is applied, stress in the X axis and Y axis is so small that they could be ignored compare with that in the Z axis. Since the whole model is a symmetrical structure, analysis is considered for just 1/4 part of the micro acclerometer and simplified model is shown in Fig.2.

According to the Hooke's law, the cantilever beam will undergo bending and a small deflections when the structure subjected to external forces. We have

$$\frac{1}{R}=\frac{M}{EI_z} \tag{1}$$

where *1/R* is the bending curvature of the cantilever beam, while *M*, *E*, and I_z refer to its bending moment, Young's modulus, and moment of inertia, respectively, and bending moment *M(x)* is obtained as

$$M(x)=M_0+Fx=ma_Z(l_b+\frac{\sqrt{2}}{2}l_m+x) \tag{2}$$

where M_0 refers to the moment of fixed end, F is the force applied to the Z axis, l_b and l_m the length of the cantilever beam and the seismic mass, respectively, and a_z the acceleration in the Z-axis.

Elastic coefficient of cantilever is

$$K_z=\frac{EI_z}{l_b}=\frac{Ew_bh_b^3}{12l_b} \tag{3}$$

where w_b and h_b refer to the width and thickness of the cantilever beam, respectively.

The charge sensitivity of the Z-axis can be derived as

$$\begin{aligned}S_q=\frac{4Q}{a_z}=&\frac{4\int_{0.5(l_b+d_1)}^{l_b}D\cdot w_b\cdot dx}{a_z}\\ &576d_{31}\cdot E_{PZT}\cdot\frac{m^2a_z(\frac{3}{2}l_b^2+\frac{\sqrt{2}}{2}l_m\cdot l_b)\cdot l_b}{E^2.w_b.(h_b+h_{PZT})^6}\\ &-576d_{31}\cdot E_{PZT}\cdot\frac{m^2a_z[0.5(l_b+d_1)l_b^2+\frac{\sqrt{2}}{4}(l_b+d_1)l_m\cdot l_b]}{E^2\cdot w_b\cdot(h_b+h_{PZT})^6}\\ &+576d_{31}\cdot E_{PZT}\cdot\frac{m^2a_z[\frac{1}{8}(l_b+d_1)^2]\cdot l_b}{E^2\cdot w_b\cdot(h_b+h_{PZT})^6}\end{aligned} \tag{4}$$

where d_{31} and E_{PZT} refer to the piezoelectric coefficient and Young's modulus of the piezoelectric PZT film, m the mass of 1/4 silicon seismic mass block, and d_1 the distance between two electrodes on the cantilever beam.

B. X/Y-axis charge sensitivity

Since the X- and Y-axis sensitivities of the micro accelerometer are the same due to the symmetric structure, only X-axis sensitivity is considered. The seismic mass rotates around the Y-axis beam because the center of the seismic mass is not in the same plane as that of the suspended beam, resulting in a rotation

angle θ (around the two Y-axis beams) and the bending moments M_a and M_b (on the two X-axis beams).

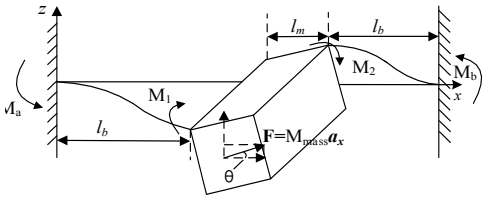

Figure 3 Simplified model with acceleration in X- or Y-axis direction

The moment of the cantilever beam:

$$\begin{aligned} M &= M_a + M_b + M_1 + M_2 \\ &= 2M_{mass} a_z \sin\theta(l_b + \sqrt{2}l_m - x) \end{aligned} \tag{5}$$

where M_{mass} is the mass of the seismic mass block. Elastic coefficient of the cantilever beam[12] ican be written as

$$K_x = \frac{(l_b^3 + \frac{3}{2}l_w \cdot l_b + \frac{3}{4}l_w^2) \cdot EI_z}{6l_b} = \frac{(l_b^3 + \frac{3}{2}l_w \cdot l_b + \frac{3}{4}l_w^2) \cdot Ew_b h_b^3}{72l_b} \tag{6}$$

The X/Y-axis charge sensitivity is obtained as

$$\begin{aligned} S_q &= \frac{Q}{a_x} = \frac{\int_{0.5(l_b+d_1)}^{l_b} D \cdot w_b \cdot dx}{a_x} \\ &= 1728 d_{31} \cdot E_{PZT} \cdot \frac{M_{mass}^2 a_x l_b \sin^2\theta[0.5(l_b - d_1)l_b]}{E^2 w_b (h_b + h_{PZT})^6 (l_b^2 + \frac{3}{2}l_w \cdot l_b + \frac{3}{4}l_w^2)} \\ &+ 1728 d_{31} \cdot E_{PZT} \cdot \frac{M_{mass}^2 a_x l_b \sin^2\theta[\frac{\sqrt{2}}{2}(l_b - d_1)l_m]}{E^2 w_b (h_b + h_{PZT})^6 (l_b^2 + \frac{3}{2}l_w \cdot l_b + \frac{3}{4}l_w^2)} \\ &- 1728 d_{31} \cdot E_{PZT} \cdot \frac{M_{mass}^2 a_x l_b \sin^2\theta[\frac{1}{8}(l_b - d_1)^2]}{E^2 w_b (h_b + h_{PZT})^6 (l_b^2 + \frac{3}{2}l_w \cdot l_b + \frac{3}{4}l_w^2)} \end{aligned} \tag{7}$$

C. Resonance frequency

In dynamic analysis, the cantilever beam is regarded as a spring mass system and the lowest resonant frequency of the tri-axis micro piezoelectric accelerometer was obtained through a Rayleigh-Ritz method [13]. When the accelerometer varies, displacement of the cantilever beam meets the equation of $z(x,t)=z(x)\sin(\omega t)$, and kinetic energy of the system can be calculated from

$$\begin{aligned} dT &= \frac{1}{2}d(M_b + M_{mass}) \cdot v^2 = \frac{1}{2}d(M_b + M_{mass}) \cdot \left[\frac{\partial z(x,t)}{\partial t}\right]^2 \\ &= \frac{1}{2}\rho w H dx[\omega \cdot z(x)\cos(\omega t)]^2 \end{aligned} \tag{8}$$

where ρ is the density of Si, and H refers to the position of cantilever beam. Potential energy of the system is

$$\begin{aligned} U &= \int_0^{2l_b + \sqrt{2}l_m} \frac{1}{2} EI_z \left[\frac{\partial^2 z(x,t)}{\partial x^2}\right] dx \\ &= \int_0^{2l_b + \sqrt{2}l_m} \frac{1}{2} EI_z [z''(x)\sin(\omega t)]^2 dx \end{aligned} \tag{9}$$

From $T=U$, we can get

$$\begin{aligned} \omega^2 &= \frac{2\int_0^{l_b} \frac{1}{2}EI_z[z''(x)]^2 dx + \int_{l_b}^{\sqrt{2}l_m} \frac{1}{2}EI_z[z''(x)]^2 dx}{2\int_0^{l_b} \rho w_b H[z(x)]^2 dx + \int_{l_b}^{\sqrt{2}l_m} \rho w_b H[z(x)]^2 dx} \\ &= \frac{E[2w_m h_m^3 + 6w_b(h_b + h_{PZT})^3]}{8[2\rho l_b^3 w_m h_m^3 + (2\sqrt{2}l_m^3 - l_b^3) \cdot (h_b + h_{PZT}) \cdot w_b]} \end{aligned} \tag{10}$$

where w_m is the width of the mass, and h_m is its thickness. Thus, the fundamental frequency is

$$\begin{aligned} f &= \frac{\omega}{2\pi} \\ &= \frac{1}{2\pi}\sqrt{\frac{E[2w_m h_m^3 + 6w_b(h_b + h_{PZT})^3]}{8[2\rho l_b^3 w_m h_m^3 + (2\sqrt{2}l_m^3 - l_b^3) \cdot (h_b + h_{PZT}) \cdot w_b]}} \end{aligned} \tag{11}$$

With the theoretically derived formulas of sensitivity and fundamental frequency above, the effects of geometrical parameters and materials properties on the performance the micro piezoelectric accelerometers can be studies. The sensitivity and resonant frequency of the device is related to length, width and thickness of cantilever beam and PZT thickness. Corresponding calculated values of the constants and the size of the parameters appearing in the equation (4), (7), (11) are given in Table 1. The relationship between them is shown in Fig.4.

The dependence of the charge sensitivity and resonant frequency of the micro accelerometer is calculated by using the analytical equations derived above. The results are plotted in Fig. 4(a-e). With the increase of thickness and width of the beam, the accelerometer charge sensitivity and resonant frequency will decrease and increase, respectively, while with the increase of the beam length, charge sensitivity and resonant frequency increases and decrease, respectively. If all the parameters are kept fixed except the PZT film thickness, it is found that an increase of the thickness of PZT caused an increase of resonant frequency increase and a decrease of charge sensitivity. As can be seen in Fig.4 (e), the charge sensitivity is proportional to the piezoelectric coefficient d_{31}, but the resonance frequency has no effect if change the piezoelectric coefficient. Thus, one way to enhance the sensitivity of the accelerometer is to raise the piezoelectric performance of the PZT thin film materials.

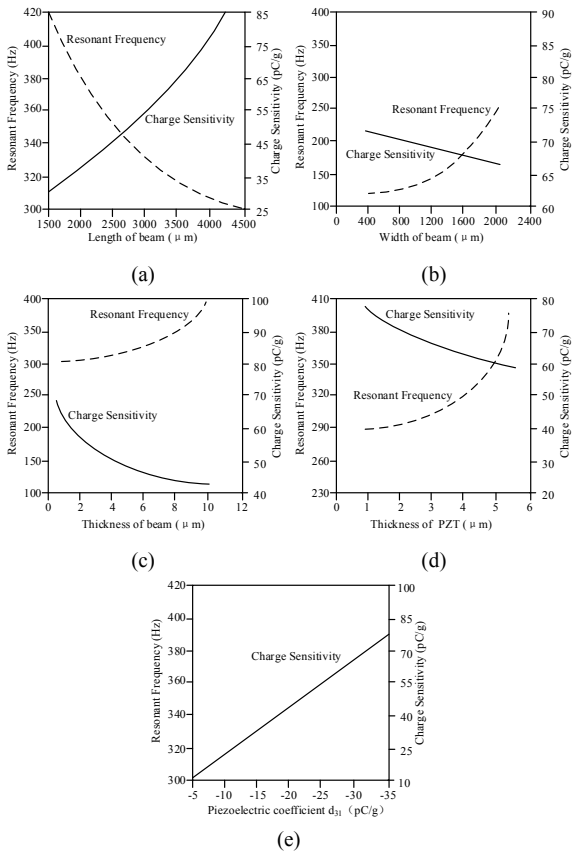

Figure 4 Performance of the micro piezoelectric accelerometer vs. structural parameters and material properties (a) Relationship between the length of the cantilever beam and the charge sensitivity and resonance frequency (b) Relationship between the cantilever beam width and the charge sensitivity and resonance frequency(c) Relationship between the cantilever beam thickness and the charge sensitivity and resonance frequency (d) Relationship between the cantilever beam thickness and the charge sensitivity and resonance frequency(e) Charge sensitivity *vs*. piezoelectric coefficient d_{31}

Table 1 Parameters of geometric size and materials properties for the design of the micro piezoelectric accelerometer

Parameter	Value
E(GPa)	120
ρ_{Si}(kg/m^3)	2330
d_{31}(pC/g)	-30
Length of mass(μm)	3970
Width of mass(μm)	3970
Thickness of mass(μm)	400
Length of beam(μm)	2010
Width of beam(μm)	1800
Thickness of beam(μm)	3
Thickness of PZT(μm)	3
Charge sensitivity of Z axis(pC/g)	67.48
Charge sensitivity of X or Y(pC/g)	9.104
Resonance frequency(Hz)	311.65

In conclusion, there is a tradeoff between the resonant frequency and sensitivity. A high resonant frequency always means a high operational range, leading to a reduction of the charge sensitivity. Conversely, high charge sensitivity and signal-to-noise ratio result in a reduced operational range.

3.2. FEM analysis

A finite element solution is used for comparison to the analytical result. Tab.1 shows the materials properties and typical dimensions of a piezoelectric accelerometer used in calculation. The piezoelectric, dielectric and elastic properties of PZT thin films reported in the literature have a strong dependence on the processing methods used to fabricate the films. Not all the necessary properties are available. When an acceleration 1g in Z direction is applied on the accelerometer, the voltage of the Z/X axis in this structure obtained by finite element method are shown in Figure 5.

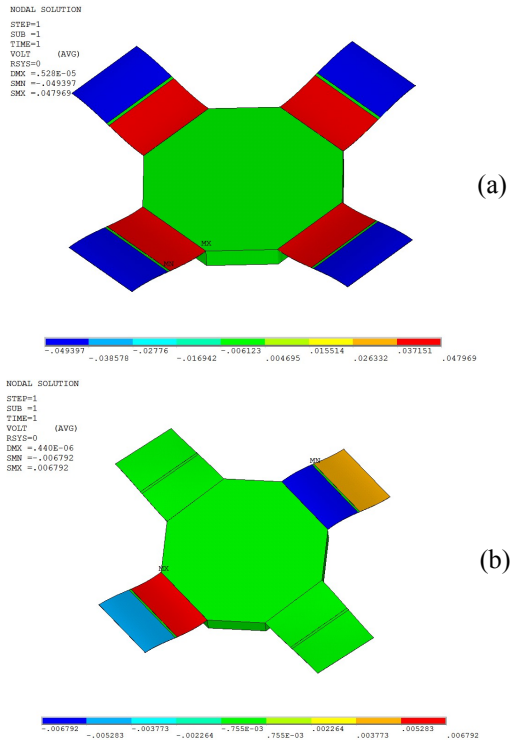

(a) Voltage/Charge distribution in Z direction.

(b) Voltage/Charge distribution in X direction.

Figure 5 Voltage/Charge distribution in Z and X direction due to the acceleration in the Z-axis and X-axis direction, respectively.

3.3. Comparison of results

Results from analytical and numerical computation are listed in Table 2 and 3. From the comparison of the analytical calculation and FEM in ANSYS shown in Table 2, it can be seen that the error of charge sensitivity is 8% while the error of the first order resonance frequency is 12%. Errors should be ascribed to that the calculation are based on some assumptions, e.g. only small deflections occur compared to their thickness, that can cause an error somewhat. Basically,

the results from analytical model are matched with the FEM results. As can be seen in Table3, for a single chip with the same chip area, the charge sensitivity of the X-shaped piezoelectric accelerometer is higher than that of the cross-shaped piezoelectric accelerometer by 21%. Therefore, the overall size of the accelerometer can be greatly reduced in the case of meeting requirements of X-shaped structure, leading to great fabrication cost reduction of each chip of the micro piezoelectric accelerometer.

Table 2 Charge sensitivity and first order resonance frequency of the X-shaped micro piezoelectric accelerometer from analytical model and FEM in ANSYS

Directions applied of accelerometer	Charge sensitivity pC/g		Resonance frequency Hz	
	Calculated values	FEM analysis	Calculated values	FEM analysis
X	9.104	8.753		
Y	9.104	8.753	311.65	355.09
Z	67.48	62.179		

Table 3 Comparison of performance of the new X-shaped and cross-shaped piezoelectric accelerometers by FEM in ANSYS

	Directions applied of accelerometer	Charge sensitivity pC/g	Resonance frequency Hz
X-shaped	X	8.753	355.09
	Y	8.753	
	Z	62.179	
Cross-shaped	X	7.398	381.13
	Y	7.398	
	Z	53.976	

4. CONCLUSIONS

In this paper, we proposed a new X-shaped piezoelectric accelerometer with tri-axial detection based on the MEMS technology. Analytical model and FEM analysis were performed to analyze the charge sensitivity and first order resonance frequency in X/Y/Z axis of the X-shaped micro piezoelectric accelerometer. The results demonstrate that in the case of a single chip with the same chip area, the charge sensitivity of the X-shaped piezoelectric accelerometer is higher than that of the cross-shaped piezoelectric accelerometer by 21%. Consequently, overall size of the accelerometer could be greatly reduced in the case of meeting the requirements of X-shaped structure.

ACKNOWLEDGMENT:

This work is financially supported by the Scientific Research and Development Program of City of Xiamen (3502Z20143003) and the Collaboration between Industry and University Program of Fujian Province (2015H6021).

REFERENCES

[1] Boxenhorn B, Greiff P. Monolithic silicon accelerometers. *Sensors and Actuators,* A21-A23, 273-277, 1990.

[2] Amarasinghe R, Dao DV, Toriyama T, Sugiyama S. Simulation, fabrication and characterization of a three-axis piezoresistive accelerometer. *Smart Materials Structure*, 15(6):1691-1699, 2006.

[3] Rudolf F. A micromechanical capacitive accelerometer with a two-point inertial-mass suspension, *Sensors and Actuators A: Physical*, Vol.4: 191-198, 1983.

[4] Tressler JF, Alkoy S, Newnham RE. Piezoelectric Sensors and Sensor Materials. *Journal of Electroceramics*, 2(4): 257-272, 1998.

[5] Ohtsuki Y, Yoshida T. Piezoelectric-ceramic biaxial accelerometer. *IOP Science*, Vol. 32, pp. 2396-2398, 1993.

[6] Zou Q, Tan W, Kim ES, et al. Single- and Triaxis Piezoelectric-Bimorph Accelerometers. *J. Micromech. Microeng.* 17(1): 45-57, 2008.

[7] Reus RD, Gulløv JO, Scheeper PR. Fabrication and characterization of a piezoelectric accelerometer. *J. Micromech. Microeng*. 9(9): 123-126, 1999.

[8] Yu. I. Iorish. Three-component accelerometer Hexemshear. *Measurement Techniques*. Vol. 38, No. 6, 649-654, 1995.

[9] Wang LP, Wang Y, Deng KK, et al. Design, fabrication, and measurement of high-sensitivity piezoelectric microelectromechanical systems accelerometers. *Journal of Microelectro- mechanical Systems*, 12(4): 433-439, 2003.

[10] Iula A, Lamberti N, Pappalardo M. Analysis and experimental evaluation of a new planar piezoelectric accelerometer. *Mechatronics, IEEE/ASME Transactions.* 4(2): 207-212, 1999.

[11] Kampen RPV, Wolffenbuttel RF. Modeling the mechanical behavior of bulk-micromachined silicon accelerometers. *Sensors and Actuators A: Physical* 64:137-150, 1998.

[12] Kollias AT, Avaritsiotis JN. A study on the performance of bending mode piezoelectric accelerometers. *Sensors and Actuators A: Physical,* 121(2): 434-442, 2005.

[13] Auld BA. Acoustic Fields and Waves in Solids. *John Wiley & Sons, pp*.357-382, 1973.